Journal of Engineering and Applied Research (JEAR)

National University of Skills

Winter & Spring 2025, Vol. 2, No. 1, p. 226-245

Journal Homepage: https://jear.tvu.ac.ir

:10.48301/jear.2025.511615.1103

Design, Fabrication and Performance Analysis of a Hybrid Multi-Stage Flash and Reverse Osmosis Desalination System

Ahmad Beytollahi Tavakoli [1], GhanbarAli Sheikhzadeh [2], Abolfazl Hajizadeh [3]

[1]Department of Mechanical Engineering, University of Kashan, Kashan, Iran

[2]Department of Mechanical Engineering, Arak University of Technology, Arak, Iran

ARTICLE INFO

Article Type:
Original Research

Received: 03.18.2025
Revised: 05.16.2025
Accepted: 10.13.2025

Keyword:
Water desalination
Multi-stage flash
Reverse osmosis
Fabrication
Performance analysis

***Corresponding Author:**
Ghanbar Ali Sheikhzadeh
Email: *Sheikhz@kashanu.ac.ir*

ABSTRACT

In this research, a freshwater production system utilizing a hybrid reverse osmosis (RO) and multi-stage flash (MSF) desalination approach has been designed and fabricated and its performance has been subjected to analysis. Initially, the RO system desalinates the saline water, and the resulting concentrated brine is fed into the MSF system. The MSF unit was tested under three distinct conditions, with the saline water inlet flow rate held constant at 0.7 liters per minute and the maximum brine temperature fixed at 82°C across all experiments. Based on relevant scientific literature and similar experimental studies, the vacuum pressures were selected to investigate the effect of chamber pressure on the overall efficiency of the system. the chamber pressures varied across the three cases: the first at ambient pressure, the second at a 5 kPa vacuum and the third at a 10 kPa vacuum. Based on the results obtained, the percentage of freshwater produced from saline water was 1.91% in the first experiment (ambient pressure), 2.40% in the second experiment (5 kPa vacuum), and 3.6% in the third experiment(10kPavacuum).

E-ISSN: 3060-6357

Introduction

Water covers 71% of the Earth's surface, with 97% being seawater [1]. Unsuitable for direct consumption, seawater leaves humanity dependent on the remaining 3% of freshwater resources. However, only 0.06% of this freshwater is readily accessible, with the majority trapped in polar ice, groundwater, and other forms [1; 2]. Lakes and rivers, though a minor fraction of surface freshwater, are vital for drinking water, agriculture, and fisheries[3; 4].Lakes constitute 87% of liquid freshwater, rivers 2%, and the rest is found in ponds and marshes [5-7].

Recent shifts in living standards, cultural practices, and population growth have escalated water consumption and Water extraction[8; 9]. Projections suggest the urban population will rise from 3.7 billion in 2010 to approximately 6.3 billion by 2050[10], while the global population is expected to increase from 7.7 billion in 2017 to about 10 billion by 2050. These trends will significantly alter freshwater use, potentially jeopardizing water security for around 3 billion people by 2050 [11]. These pressures have driven global efforts to address water scarcity, with desalination emerging as a historical solution.

Borsani et al. (2005) conducted a study to examine and compare the costs and technological principles of water desalination using the multi-stage flash (MSF) method with other technologies. According to their findings, the MSF method, due to its reliable process and ability to operate over extended periods, has captured a significant share of the Middle Eastern market. The installation costs of MSF systems have decreased in recent years due to improved designs and an increase in the number and capacity of units. Additionally, factors such as competition, technical optimization, and contracts for construction, ownership, operation, and transfer have contributed to reducing the installation costs of these systems. Furthermore, standardized designs and the use of more durable and cost-effective materials, such as duplex steel, have aided in this cost reduction. Ultimately, they compared the cost of water production using the MSF method with reverse osmosis and multi-effect distillation (MED), concluding that the production costs of these three methods are quite similar, although reverse osmosis is slightly more cost-effective. Nevertheless, due to the compatibility of the MSF method with the specific needs of the Middle East, this technology continues to be well-received in the region [12].

Alhazmy et al. (2014) investigated the thermal and economic feasibility of a water desalination system employing the MSF method with brine-feed cooling. A key issue in this technology is the reduction of inlet water temperature during summer, which enhances condensation and improves system performance. To achieve this, a cooling system was incorporated at the inlet to bring the water

temperature to an optimal range. Their results indicate that adding a cooler and mixing chamber increases initial and operational costs, but the enhanced freshwater production offsets these expenses. Overall, this technology not only improves efficiency but is also deemed economically viable for hot regions, particularly in countries like Saudi Arabia [13].

Bandi et al. (2016) focused on optimizing hybrid seawater desalination processes using the MSF and reverse osmosis methods. Employing a differential evolution algorithm, they analyzed several hybrid MSF-RO configurations to minimize freshwater production costs. Five different configurations of this hybrid system were simulated and compared using various optimization techniques, such as sequential quadratic programming and other methods. In this study, the freshwater production cost for the fourth hybrid configuration was the lowest, at $0.9703 per cubic meter, and was selected as the optimal configuration. Their findings demonstrate that the differential evolution algorithm, due to its capability to solve nonlinear problems, provides superior optimization results compared to other methods, making it the most suitable choice for designing MSF-RO systems [14].

Darawsheh et al. (2019) explored the optimization of a solar-powered water desalination process using the MSF system and constructed a prototype of this system. In their research, flat-plate solar collectors were used to heat saline water, and vacuum conditions were applied across multiple stages. This approach resulted in a 53% increase in the distillate-to-evaporation ratio and a 35% reduction in energy consumption. By reducing the vacuum pressure to 20 kPa, the system reached its optimal performance. Additionally, experiments revealed that the distillation rate could be controlled under varying pressures and inlet water flow rates, with the evaporation-to-distillation ratio improving as the flow rate decreased. Consequently, this system was determined to be suitable for reducing costs and enhancing the sustainability of solar-powered desalination processes [15].

Babaee et al. (2021) designed and evaluated a solar-powered MSF desalination unit utilizing a parabolic dish collector and a vacuum pump. This study examined the effects of varying saline water flow rates and vacuum pressures on water production. The highest output, 3.22 liters over 5 hours, was achieved at a flow rate of 0.7 liters per minute and a vacuum pressure of 10 kPa. The results showed that increasing the flow rate reduced production by 76.4%, while decreasing pressure improved efficiency by 34%. The exergy efficiency of the MSF unit was very low (0.07%), with significant energy losses occurring across the stages. Based on economic analysis, the production cost for a capacity of 8,000 liters per day was reduced to $1.5 per cubic meter [16].

Thabit et al. (2022) addressed the design and modeling of a water desalination process using the MSF technology. They developed a model in Excel to assess the energy requirements for operating a 16-stage MSF system and optimized its performance by adjusting parameters. Simulations indicated that a steam flow rate of 29.5 kg/s was required to desalinate 162 kg/s of water, with an initial saline water temperature of 130°C. The results highlighted a performance ratio decline from 5.49 to 2.66 as the inlet water temperature dropped from 30°C to 5°C. The precise modeling in Excel and simulations in Epsilon software enabled economic and performance predictions, aiding the optimization of the MSF unit [17].

Harby et al. (2024) investigated various water desalination methods, particularly the integration of reverse osmosis with other technologies, to address water scarcity challenges. As reverse osmosis faces issues due to high energy demands and the production of concentrated brine, this study explored hybrid approaches and their impacts on overall water treatment system performance. The strengths and weaknesses of different desalination methods were evaluated. The findings suggest that hybrid systems can enhance freshwater production ratios, reduce energy consumption, and mitigate the environmental issues associated with concentrated brine discharge. Analyses revealed that hybrid MSF-RO systems achieved daily water production ranging from 14.4 to 1,000 cubic meters with lower energy use. Despite the significant advantages of hybrid systems, challenges such as integration complexities and increased maintenance requirements persist. Overall, this research emphasizes that hybrid RO systems can address the limitations of standalone methods, offering an economically and environmentally efficient solution for freshwater production [18].

Based on the review of studies concerning freshwater production methods, particularly those related to the MSF technique, it is evident that this method, whether used independently or in combination with other approaches, can effectively produce freshwater. Although these studies have been conducted from various perspectives, achieving an efficient technology requires further investigation. Therefore, in this research, a three-stage MSF system integrated with a reverse osmosis system has been designed and fabricated, and its performance has been examined and thermodynamically analyzed through various experiments.

Experimental System Description

Figure 1 provides a complete view of the fabricated desalination system unit, while Figure 2 presents a schematic representation of it. The system consists of two distinct sections: the first is the reverse osmosis (RO) desalination unit, and

the second is the multi-stage flash (MSF) desalination unit. In the RO desalination process, salt particles in saline water are separated as the water passes through a semi-permeable membrane, resulting in freshwater production. Naturally, flow typically occurs from a dilute solution to a concentrated one, a process known as osmosis. However, in reverse osmosis, the flow is directed from saline water (concentrated solution) to freshwater (dilute solution) under external pressure, with the membrane removing impurities as the water passes through [19].

In the RO desalination section, a six-stage desalination device is employed, comprising a pre-treatment filter, an activated carbon filter, a carbon block filter, an RO membrane filter, a post-carbon filter, and an alkaline filter. This system received 300 liters of saline water over a 24-hour period, ultimately delivering 140 liters of freshwater and producing 160 liters of concentrated brine. The RO membrane used in this study is a thin-film composite (TFC) polyamide membrane with a maximum capacity of 300 liters per day (approximately 80 GPD), a salt rejection rate of approximately 98%, and an operating pressure range of 4 to 7 bar. This small-scale RO unit is integrated into a six-stage filtration system, as described above.

Figure 1. Desalination System Unit.

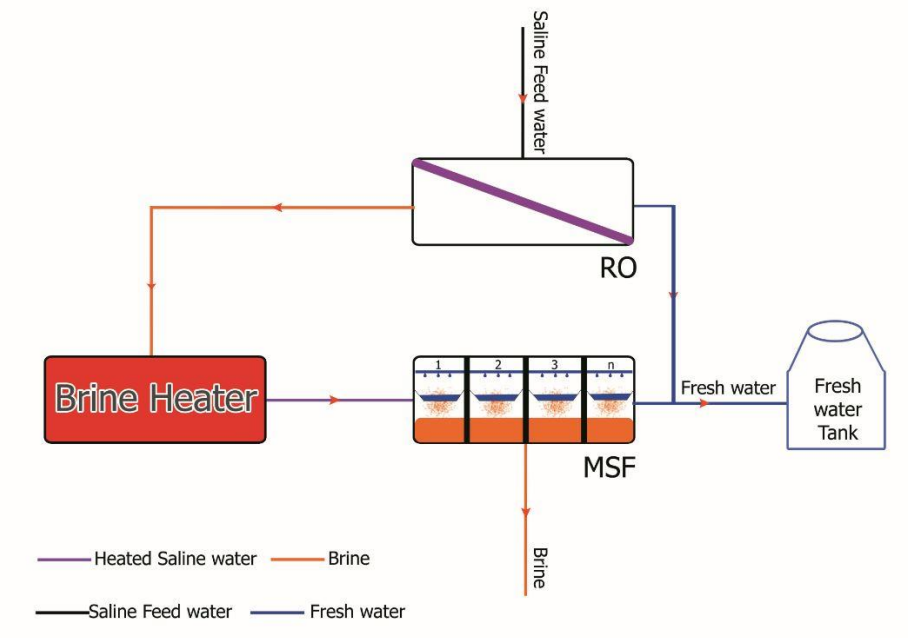

Figure 2. Schematic view of the Desalination System Unit.

The brine (concentrated water) discharged from the first section (RO) enters the second desalination section, the MSF unit. Figure 3 provides a schematic view of the MSF desalination unit. The MSF method is a heat-based water desalination technique wherein saline water is evaporated and subsequently condensed within the system to produce freshwater [20].

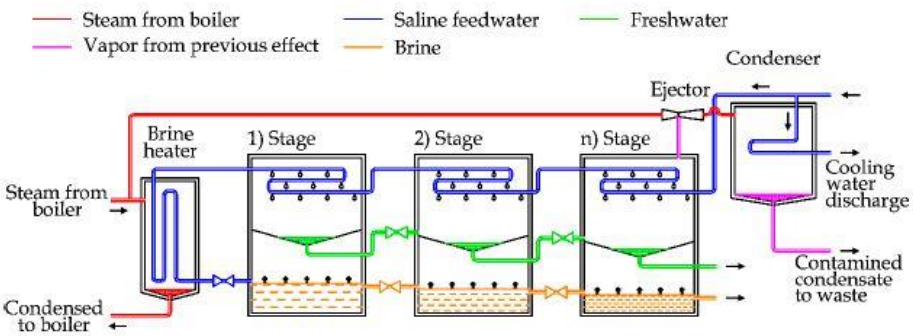

Figure 3. Multi-Stage Flash Desalination Unit [20].

As depicted in Figure 3, saline water first enters chamber n and passes through condensers before exiting chamber 1. During this stage, the saline water is heated, raising its temperature, and then enters the first chamber and brine chamber from the bottom. At this point, due to the pressure difference between the chambers and the ambient pressure—created by a vacuum pump—the heated saline water undergoes sudden evaporation, a phenomenon termed flash evaporation. The water vapor rises to the top of the chamber, contacts the condenser, condenses, and drips into the freshwater collection tank. The remaining unevaporated saline water proceeds to the second chamber, where the process repeats, continuing through to chamber n. Ultimately, the concentrated brine is transferred to a discharge collection site, which could be the sea, evaporation ponds, or similar locations.

In the fabricated system, the MSF desalination unit consists of three chambers. Figure 4 illustrates both a schematic and a real view of these chambers, each constructed from 4 mm thick steel sheets with dimensions of 100 × 34 × 80 cm (length, width, and height). Each chamber features one inlet and one outlet for saline water to the condenser, one freshwater outlet (3/4 inch), one inlet and one outlet for heated saline water (2 inches), an air outlet, and a chamber drainage outlet (1/2 inch).

Figure 4. Schematic and Real View of the Desalination System Chambers.

Each chamber is equipped with a condenser rated at 30,000 Btu/hr, measuring 20 × 60 cm, featuring 3/8-inch copper tubing and aluminum fins with a density of 8 fins per inch, and including 3/4-inch inlets and outlets. Figure 5 depicts this condenser.

Each chamber also includes a freshwater collection tank made from 4 mm thick mild steel sheets, designed with a sloped geometry to optimize collection efficiency. To enhance corrosion and rust resistance, the internal and external surfaces were coated with a heat-cured industrial paint.

Figure 6 shows the collection tank and condenser positioned within the chamber.

The total fabrication cost of the system was estimated at approximately $3,200, covering raw materials (steel sheets, copper tubing, filters), sensors, the vacuum pump, and control systems. Routine maintenance includes cleaning RO membranes every 3 months and descaling MSF chambers biannually. Energy consumption includes an 80,000 kcal/h gas burner for heating, a 0.5 hp (370 W) circulation pump for water flow, an RO unit consuming approximately 48 W of electricity, and a vacuum pump consuming approximately 250 W. While electricity costs can be significant, the system can be solar-powered as discussed in section 2.2

Figure 5. Condenser of the Desalination System Unit.

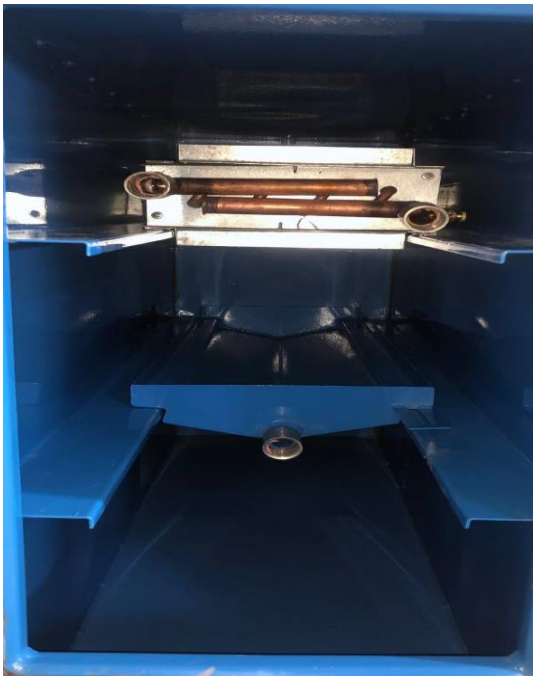

Figure 6. Freshwater Collection Tank of the Multi-Stage Flash Desalination Unit.

Governing equations

Based on the assumptions and conditions of the problem, the energy analysis of the water desalination system is conducted using energy conservation equations. Additionally, mass conservation equations are applied to water, vapor, and salt. The general forms of the mass and energy conservation equations are expressed as follows:

$$\sum \dot{m}_{in} = \sum \dot{m}_{out} \quad (1)$$

$$\sum_{out} \dot{m} \times h - \sum_{in} \dot{m} \times h = \dot{Q}_{cv} - \dot{W}_{cv} \quad (2)$$

$$\sum \dot{m}_{in} \times X_{in} = \sum \dot{m}_{out} \times X_{out} \quad (3)$$

In the above equations, $\dot{m}$, h, $\dot{Q}_{cv}$, $\dot{W}_{cv}$ and X denote the flow rate, specific enthalpy, heat transfer rate, work rate and concentration, respectively.

The brine entering the first stage absorbs heat from a heater, calculated according to Equation (4):

$$Q_{in_s} = m_A C_{ps}\left(T_A - T_{sat_{steam}}\right) + m_A h_{fg} \quad (4)$$

Due to the presence of impurities in saline water, Equation (5) is used to determine the temperature within a range of 10 to 180°C and a total dissolved solids (TDS) concentration range of 1 to 160,000 ppm [21]:

$$T_i = T_{\text{sat}_i} + \text{BPE} \quad (5)$$

Here, BPE represents the boiling point elevation of the incoming brine, calculated using Equations (6) to (9):

$$\text{BPE} = X(A + \text{BX} + \text{CX}^2) \quad (6)$$

$$A = 8.325E-2 + 1.833E-4 \times T_i + 4.02E-6 \times {T_i}^2 \quad (7)$$

$$B = -7.625E-4 + 9.02E-5 \times T_i - 5.2E-7 \quad (8)$$

$$\boldsymbol{C = 1.522E-4 - 4E-6 \times T_i - 3E-8 \times T_i^2} \quad (9)$$

In each stage, the distilled vapor is converted to liquid through heat transfer with condensers carrying the incoming brine flow. The required heat transfer area is obtained from Equation (10):

$$A(i) = \frac{m_{s_1} h_{fgf}}{(U_i(T_1 - T_2))} \quad (10)$$

In this equation, Ui is the overall heat transfer coefficient for each stage, calculated as follows:

$$U(i) = 1.6175 + 1.537E-4(T_i) - 1.825E-4(T_i)^2 + 8.026E-8(T_i)^3 \quad (11)$$

As explained, a portion of the saline water is desalinated, and the remaining saline water, with a reduced temperature, is transferred to the next stage. The temperature of the final stage is determined using Equation (12), and the temperature difference between consecutive stages is calculated using Equation (13) [22]:

$$T_{st.m} = T_{\text{ambient}} + 10 \quad (12)$$

$$\Delta T = \frac{(T_1 - T_{st.m})}{n} \quad (13)$$

The efficiency percentage of the MSF system is calculated using the following equation:

$$\text{Efficiency Percentage} = \frac{\text{Fresh Water (Kg)}}{\text{Saline Feed Water (Kg)}} \times 100\% \quad (14)$$

Control and Data Acquisition

The system includes a gas burner with a capacity of 80,000 kcal/hr, responsible for producing hot water. This burner uses a sensor placed inside the tank to automatically control the saline water temperature, maintaining it between 80 and 85°C.

A vacuum pump is tasked with reducing the pressure within the chambers. As shown in Figure 1, this pump is connected in parallel to the chambers and reduces

the internal air pressure based on a preset value. The pump operates under the command of a pressure sensor; once activated, it reduces the pressure to the specified value on the control board and then shuts off. It automatically restarts whenever the chamber pressure exceeds the set value by 3 kPa. Given that the experiments were conducted under three different pressure conditions, the set values were ambient pressure for the first case, 75 kPa for the second, and 70 kPa for the third.

In the experimental system, temperature is measured at 12 points using digital resistance thermometers with a measurement range of -55 to 125°C and an accuracy of ±0.05°C. At the inlet of the first chamber, a flow meter capable of measuring flow rates from 0.03 to 30 liters per minute is installed. Chamber pressure is monitored by a digital pressure sensor with a measurement range of 300 to 1,100 hPa and an accuracy of ±1 hPa. Figure 7 illustrates the pressure sensor, flow meter, and one of the temperature sensors along with its sheath.

Figure 8 provides a schematic view of the sensor placements and the custom-designed software used to control them. This software displays 150 data points per minute, stored as an Excel file, and indicates the on/off status of the water circulation pump, heater, vacuum pump, and solenoid valve. The sensors collect data via a control Panel, shown in Figure 9, which is displayed on a monitor and transmitted to the data acquisition system via a network cable.

Iran has an average annual solar radiation of 2200 KWh/m^2, and 90% of the country has enough sunlight to produce solar energy in 300 days of the year that this ideal condition can be used to supply electricity and heat for all the mentioned equipment of this system using solar energy[23].

Figure 7. Pressure Sensor, Temperature Sensor and Flow Meter of the Experimental System.

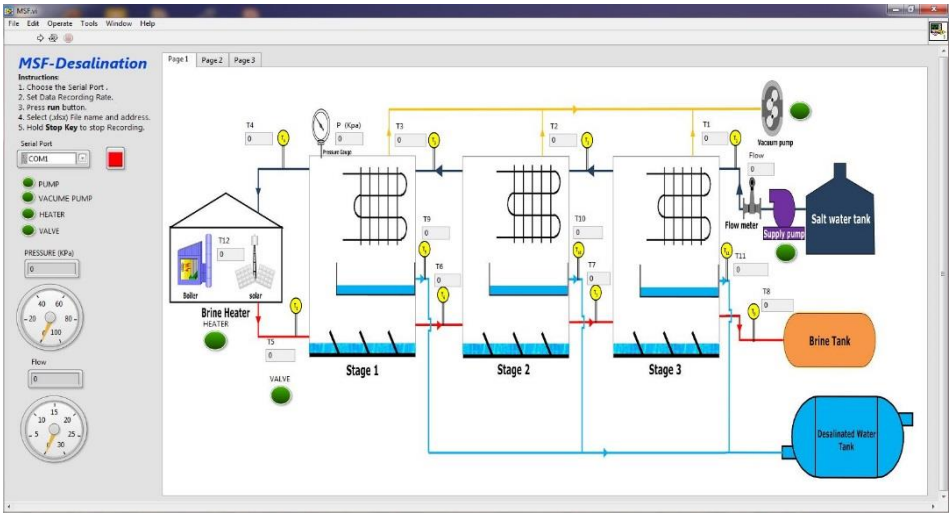

Figure 8. Schematic View of the Measurement Device Control Software.

Figure 9. Control Panel for Measurement Devices of the Experimental System.

Results and Discussion

In this study, based on relevant scientific literature and similar experimental studies, the vacuum pressures were selected to investigate the effect of chamber pressure on the overall efficiency of the system, experiments were conducted under three chamber pressure conditions: ambient pressure, a 5 kPa vacuum, and a 10 kPa vacuum. In all three cases, the saline water flow rate was constant at 0.7 liters per minute, and the maximum saline water temperature (Top Brine

Temperature) was set at 82°C. The ambient pressure at the experiment location was measured as 82.54 kPa.

Temperature measurements at 12 points provided highly precise data regarding the inlet and outlet temperatures of each chamber's condenser, as well as the inlet and outlet temperatures of the heated saline water for each chamber. This data can be utilized for calculations related to water vapor condensation, as well as energy, exergy, environmental, and economic analyses of desalination systems. It also enables the examination of the relationship between freshwater production in each stage and its correlation with the temperature of the inlet saline water and heated saline water, as well as process analysis in systems with a greater number of stages.

Figure 10 presents a graph of the temperature readings from sensors 1 to 8 for the first experiment (ambient pressure) from the start to the end of the experiment. The duration of this experiment was 172 minutes, with the inlet saline water temperature at 19°C. Over this period, 120.4 liters of saline water with a salinity of 7,000 ppm entered the system, resulting in 2.3 liters of freshwater with a salinity of 48 ppm and a temperature of 29°C by the end of the experiment

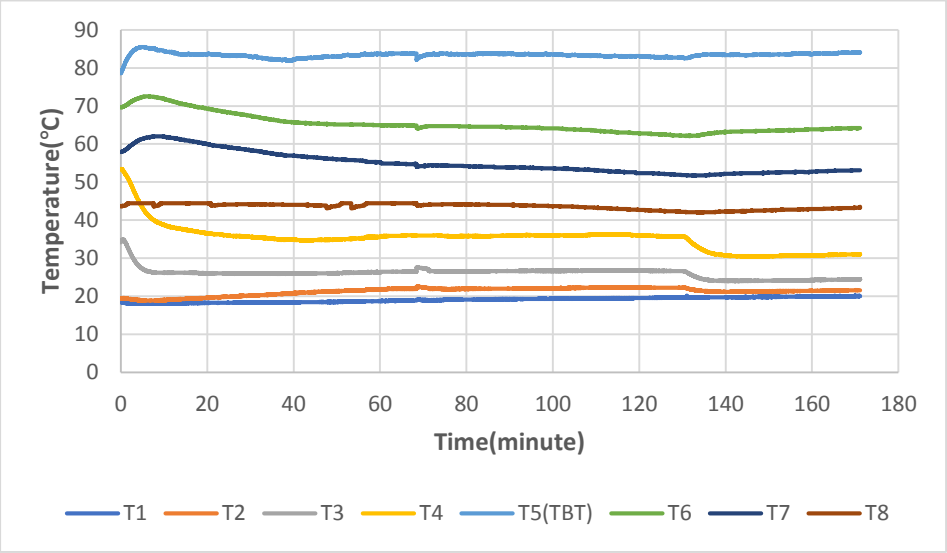

Figure 10. Temperature Variations of Sensors 1 to 8 in the First Experiment.

Figure 11 displays a graph of the temperature readings from sensors 1 to 8 for the second experiment (5 kPa vacuum) as a function of experiment duration. This experiment lasted 146 minutes, with an inlet saline water temperature of 21°C. Using the vacuum pump, the air pressure inside the chambers was reduced by 5

kPa below ambient pressure. Over the experiment duration, with a flow rate of 0.7 liters per minute, 102 liters of saline water with a salinity of 7,000 ppm entered the system, resulting 2.45 liters of freshwater with a salinity of 54 ppm and a temperature of 28°C.

Figure 12 shows a graph of the temperature readings from sensors 1 to 8 for the third experiment (10 kPa vacuum) from the start to the end of the experiment. This experiment lasted 163 minutes, with saline water entering at a flow rate of 0.7 liters per minute and a temperature of 22.65°C. In this case, the vacuum pump reduced the chamber pressure by 10 kPa below ambient pressure. Over the experiment duration, 114 liters of saline water with a salinity of 7,000 ppm entered the system, producing 4.1 liters of freshwater with a salinity of 34 ppm and a temperature of 31°C.

The disposal of the discharge brine is one of the major challenges in desalination systems. In this system, we disposed of the discharge brine through the sewage; however, at larger scales, this approach will undoubtedly face serious challenges. Therefore, examining brine disposal methods and selecting the best option is essential for the design of a desalination system. Additionally, due to its hybrid nature and thermal process, this system has the potential for upgrading to achieve zero liquid discharge (ZLD).

Figure 13 illustrates the pressure variations within the chambers during the second and third experiments over their respective durations. The second experiment lasted 146 minutes, and as observed, the vacuum pump activated multiple times within the first 25 minutes to establish a 5 kPa vacuum.

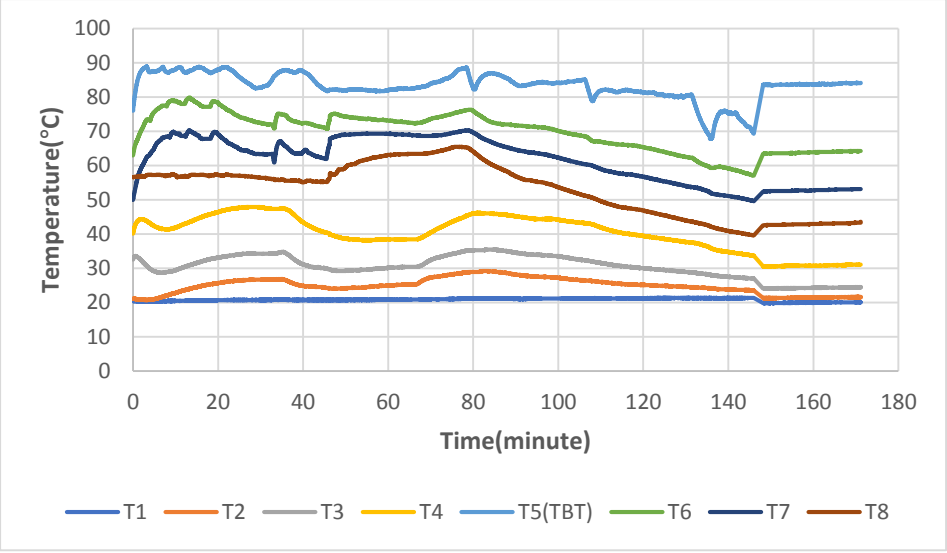

Figure 11. Temperature Variations of Sensors 1 to 8 in the Second Experiment.

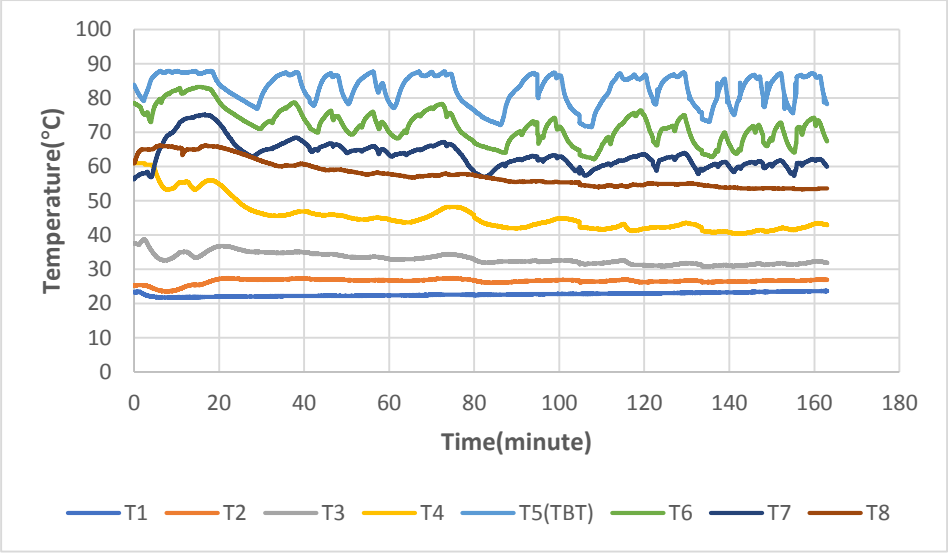

Figure 12. Temperature Variations of Sensors 1 to 8 in the Third Experiment.

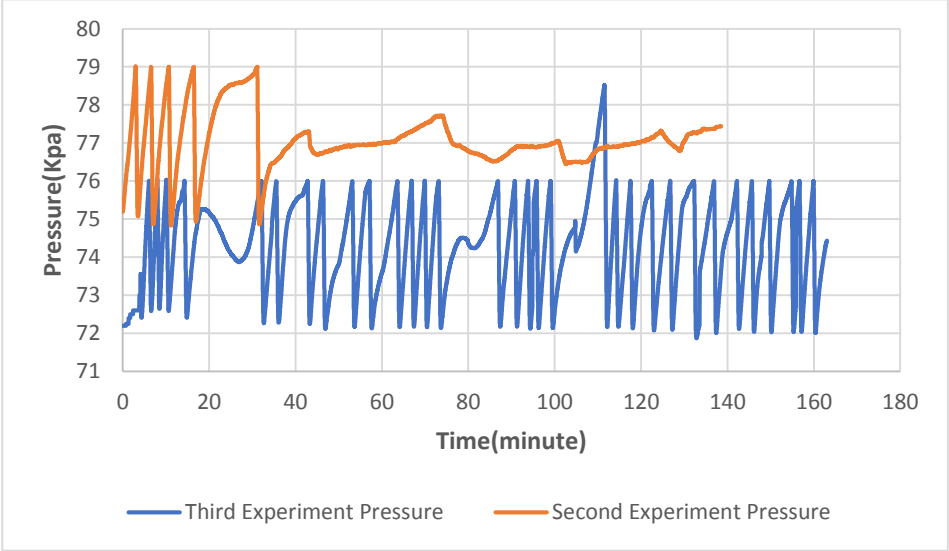

Figure 13. Pressure Variations in the Chambers During the Second and Third Experiments.

However, after a period, with vapor generation in the chambers and temperature stabilization, the pressure inside the chambers stabilized, eliminating the need for further pump activation. The third experiment lasted 163 minutes, and as evident, maintaining a 10 kPa vacuum required continuous operation of the vacuum pump, as sustaining this pressure level was challenging for the system, with the vacuum frequently dissipating.

Figure 14 depicts the temperature changes of the saline water passing through the condensers from its entry into the first condenser to its exit from the third condenser. As observed, the temperature of the water entering the condenser increases as it passes through it. This is due to the continuous contact of the saline water vapor, evaporated in the chambers, with the condensers. The temperature increase slope is steeper when passing through the third condenser compared to the previous two, as the vapor temperature in the third condenser (first chamber) is significantly higher than in chambers 2 and 3.

Figure 15 illustrates the temperature changes of the heated saline water from its entry into the first chamber to its exit from the third chamber. As shown, the 82°C water entering the first chamber decreases in temperature as it passes through the chambers due to heat exchange with the environment and evaporation. However, the graph indicates that the greater the applied vacuum pressure, the less the temperature decreases. Specifically, a 42°C temperature drop occurs at ambient pressure, a 30°C drop at a 5 kPa vacuum, and a 25°C drop at a 10 kPa vacuum.

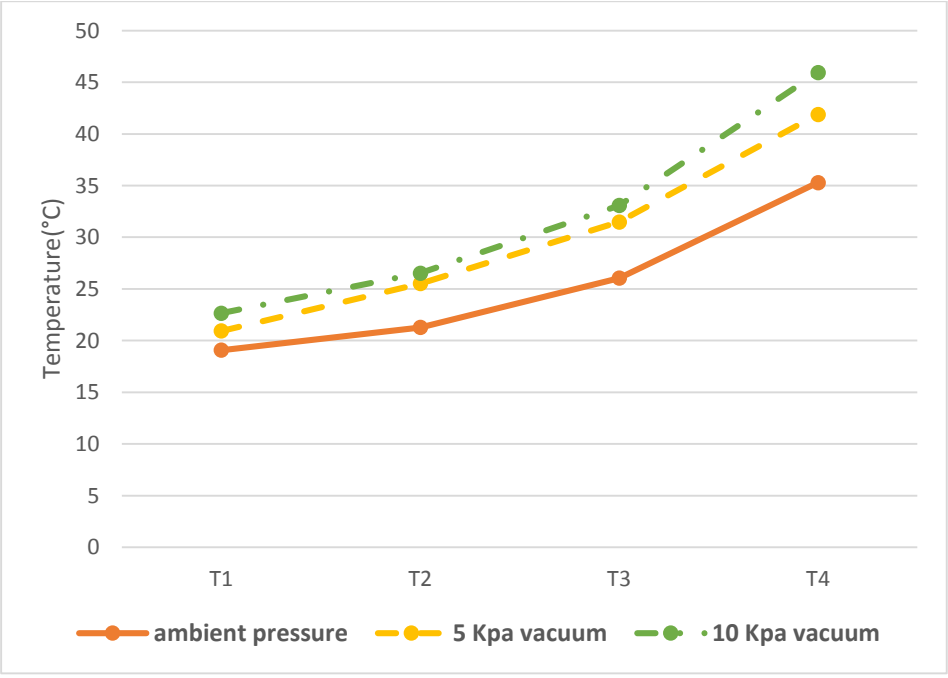

Figure 14. Temperature Changes of Saline Water Passing Through the Condensers.

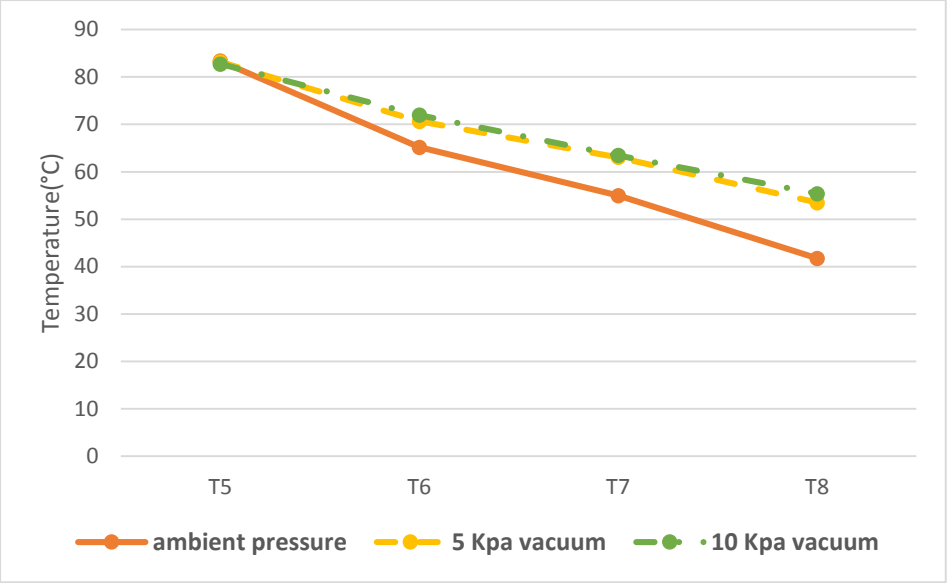

Figure 15. Temperature Changes of Heated Saline Water Passing Through the Chambers.

Table 1 presents the efficiency percentage of the MSF desalination system (current system) based on Equation (14), along with the average sensor temperatures, chamber pressures, and flow rates for the three experimental conditions. The efficiency percentage and average temperature of each sensor are used in the relevant equations and provide a concise and comprehensive overview of the experimental system's status. As observed, reducing the pressure within the chambers (due to a lower water evaporation temperature and increased evaporation in the chambers) enhances the system's efficiency percentage. Accordingly, the freshwater production percentage from saline water (efficiency) was 1.91% in the first experiment (ambient pressure), 2.40% in the second experiment (5 kPa vacuum), and 3.6% in the third experiment (10 kPa vacuum). Thus, reducing chamber pressure while maintaining a constant maximum saline water temperature (82°C) and flow rate (0.7 liters per minute) significantly increases the efficiency of the MSF system. A 5 kPa pressure reduction in the chambers increased efficiency by 26%, while a 10 kPa reduction improved it by 88% compared to ambient pressure.

It is noteworthy that the present results, compared to those of similar previous studies, demonstrate the satisfactory performance of the current system. For instance, Darawsheh et al. [15], using a two-chamber MSF desalination system with flat-plate solar collectors for heating, achieved an efficiency of 2.8% at a saline water flow rate of 0.5 liters per minute and a 10 kPa vacuum chamber pressure. Similarly, Babaee et al. [16], employing a two-

chamber MSF desalination system with solar energy, produced 3.22 liters of freshwater from 210 liters of saline water at a flow rate of 0.7 liters per minute, a 10 kPa vacuum, and a maximum saline water temperature of 94.25°C, indicating an efficiency of 1.53%.

Therefore, the system designed and fabricated in this study exhibits 30% higher efficiency than that of Darawsheh et al. and 135% higher efficiency than that of Babaee et al. It is anticipated that further improvements in the freshwater collection chamber and insulation of the chambers could enhance the performance of the current system even more.

It should be noted that Hybrid systems offer the flexibility to integrate and optimize specific processes that complement each other effectively[24].

Table 1. System Efficiency and Average Measured Quantities Across Three Experimental Stages.

Quantity	Experiment 1 (Ambient Pressure)	Experiment 2 (5 Kpa Vacuum)	Experiment 2 (10 Kpa Vacuum)
Efficiency(%)	1.91	2.4	3.6
T1°C	19.07	20.93	22.65
T2°C	21.27	25.51	26.53
T3°C	26.04	31.48	33.08
T4°C	35.28	41.88	45.94
T5°C	83.39	83.19	82.72
T6°C	65.20	70.64	71.96
T7°C	54.99	63.05	63.45
T8°C	41.74	53.50	55.41
Pressure(Kpa)	82.54	77.05	72.55
Flow Rate(l/m)	0.7	0.7	0.7

Conclusion

In this study, a freshwater production system employing a hybrid multi-stage flash (MSF) and reverse osmosis (RO) method was designed and fabricated, and its performance was thermodynamically analyzed. The desalination of saline water with a salinity of 7,000 ppm was tested under three conditions: the first at ambient pressure, the second at a 5 kPa vacuum, and the third at a 10 kPa vacuum. The resulting freshwater had a salinity of less than 55 ppm, indicating high desalination quality. Based on the obtained results, the efficiency of the fabricated system for freshwater production was 1.91% at ambient pressure, 2.40% at a 5 kPa vacuum, and 3.6% at a 10 kPa vacuum. Therefore, reducing chamber pressure (while keeping the flow rate and maximum saline water temperature constant) significantly enhanced the efficiency of the MSF system. A 5 kPa reduction in chamber pressure increased efficiency by 26%, and a 10 kPa reduction improved it by 88%.

Disclosure statement and funding

The authors declare no potential conflicts of interest. This research was conducted with financial support from the Iran Small Industries and Industrial Parks Organization.

Acknowledgment

The authors wish to thank the Iran Small Industries and Industrial Parks Organization. Also, the authors wish to thank the Energy Research Institute and the Research & Technology Administration of the University of Kashan for their support regarding this research.

References

[1] Ahuja, S. (2009). *Handbook of water purity and quality*. Academic press.

[2] Rijsberman, F. R. (2006). Water scarcity: fact or fiction? *Agricultural water management*, *80*(1-3), 5-22. https://doi.org/10.1016/j.agwat.2005.07.001

[3] Adamowski, J., & Sun, K. (2010). Development of a coupled wavelet transform and neural network method for flow forecasting of non-perennial rivers in semi-arid watersheds. *Journal of Hydrology*, *390*(1-2), 85-91. https://doi.org/10.1016/j.jhydrol.2010.06.033

[4] Lerman, A., Imboden, D. M., Gat, J. R., & Chou, L. (1995). *Physics and chemistry of lakes*. Springer-Verlag Berlin.

[5] El-Dessouky, H. (2002). *Fundamentals of Salt Water Desalination*. Elsevier.

[6] El-Ghonemy, A. (2012). Future sustainable water desalination technologies for the Saudi Arabia: a review. *Renewable and Sustainable Energy Reviews*, *16*(9), 6566-6597. https://doi.org/10.1016/j.rser.2012.07.026.

[7] Grphics, U. V. W. (2002). An Overview of the State of the World's Fresh and Marine Water. *United Nation Environment Programme. Nairobi, Kenya*.

[8] Miller, J. E. (2003). *Review of water resources and desalination technologies*.

[9] Qu, X., Brame, J., Li, Q., & Alvarez, P. J. (2013). Nanotechnology for a safe and sustainable water supply: enabling integrated water treatment and reuse. *Accounts of chemical research*, *46*(3), 834-843. https://doi.org/10.1021/ar300029v

[10] Haddout, S., Priya, K. L., Hoguane, A. M., & Ljubenkov, I. (2020). Water scarcity: A big challenge to slums in Africa to fight against COVID-19. *Science & Technology Libraries*, *39*(3), 281-288. https://doi.org/10.1080/0194262X.220.1765227

[11] UNWWD, Nature-Based Solutions for Water Paris, 2018.

[12] Borsani, R., & Rebagliati, S. (2005). Fundamentals and costing of MSF desalination plants and comparison with other technologies. *Desalination*, *182*(1-3), 29-37. https://doi.org/10.1016/j.desal.2005.03.007

[13] Alhazmy, M. M. (2014). Economic and thermal feasibility of multi stage flash desalination plant with brine–feed mixing and cooling. *Energy*, *76*, 1029-1035. https://doi.org/10.1016/j.energy.2014.09.022

[14] Bandi, C. S., Uppaluri, R., & Kumar, A. (2016). Global optimality of hybrid MSF-RO seawater desalination processes. *Desalination*, *400*, 40-45. https://doi.org/10.1016/j.desal.2016.04.012

[15] Darawsheh, I., Islam, M., & Banat, F. (2019). Experimental characterization of a solar powered MSF desalination process performance. *Thermal Science and Engineering Progress*, *10*, 154-162. https://doi.org/10.1016/j.tsep.2019.01.018

[16] Babaeebazaz, A., Gorjian, S., & Amidpour, M. (2021). Integration of a solar parabolic dish collector with a small-scale multi-stage flash desalination unit: experimental evaluation, exergy and economic analyses. *Sustainability*, *13*(20), 11295. https://doi.org/10.3390/su132011295

[17] Thabit, Q., Nassour, A., & Nelles, M. (2022). Water Desalination Using the Once-through Multi-Stage Flash Concept: Design and Modeling. *Materials*, *15*(17), 6131. https://doi.org/10.3390/ma15176131

[18] Harby, K., Emad, M., Benghanem, M., Abolibda, T. Z., Almohammadi, K., Aljabri, A., Alsaiari, A., & Elgendi, M. (2024). Reverse osmosis hybridization with other desalination techniques: An overview and opportunities. *Desalination*, 117600. https://doi.org/10.1016/j.desal.2024.117600

[19] El Aimani, S. (2023). Modeling of reverse osmosis water desalination powered by photovoltaic solar energy. *Green Energy and Environmental Technology*. https://doi.org/10.5772/GEET.15

[20] Buros, O. (2000). *The ABCs of desalting* (Vol. 2). International Desalination Association Topsfield, MA.

[21] Tayyeban, E., Deymi-Dashtebayaz, M., & Gholizadeh, M. (2021). Investigation of a new heat recovery system for simultaneously producing power, cooling and distillate water. *Energy*, *229*, 120775. https://doi.org/10.1016/j.energy.2021.120775

[22] Deymi-Dashtebayaz, M., & Tayyeban, E. (2019). Multi objective optimization of using the surplus low pressure steam from natural gas refinery in the thermal desalination process. *Journal of Cleaner Production*, *238*, 117945. https://doi.org/10.1016/j.jclepro.2019.117945

[23] Mofidian, R., Hassankhani, I., Jahanshahi, M., Hosseini, S. S., & Miansari, M. (2024). Cost Effective Design of a 200 kW On-grid Rooftop Photovoltaic System Using PVsyst Software in Shiraz. *Journal of Engineering and Applied Research (JEAR)*, *1*(1), 13-24. https://doi.org/10.48301/JEAR.2024.194109

[24] Jahanshahi, M., Mofidian, R., & Hakimzadeh, M. (2024). Membrane Distillation Configurations and Hybrids: A Review. *Journal of Engineering and Applied Research (JEAR)*, *1*(2), 13-27. https://doi.org/10.48301/JEAR.2024.421746.1006